JOURNAL OF COLLOID AND INTERFACE SCIENCE 160, 405–418 (1993)

Coagulation of Particles in Shear Flow: Applications to Biological Cells

ANDREW A. POTANIN,[1] VLADYSLAV V. VERKHUSHA, AND PETER V. VRZHESHCH*

*Department of Chemistry and *Belozersky Institute of Physicochemical Biology, Moscow State University, Moscow 119899, Russia*

Received May 20, 1992; accepted April 15, 1993

A simplified model is developed which makes it possible to describe the shear-induced coagulation of particles with different types of attractive interactions. In this model the trajectories of particles are calculated without taking into account any nonhydrodynamic interactions, while the hydrodynamic interaction is described in terms of the lubrication theory. Coagulation is assumed to occur if the hydrodynamic stretching force exerted on the doublet of particles is smaller than the attractive force binding the particles together. If the nonhydrodynamic interaction is reduced to the Van der Waals forces of molecular attraction, calculations of capture efficiency in terms of our simplified analysis are shown to be in good agreement with those carried out by other authors on the basis of analysis of numerically calculated trajectories. Further applications of our model deal with the coagulation of some biological cells, namely blood platelets, which are responsible for thrombous formation. In the first approximation activated platelets can be described as spherical elastic particles interacting via the superposition of Van der Waals attraction and biochemically specific interactions, which are attributed to receptor–coreceptor bonds between cells. The specific interactions are considered to result from the interplay of two subsystems, chemical and mechanical ones. The analysis of the kinetics of formation of intercellular bonds is carried out, yielding a simple analytic representation for the force of biospecific interaction. The biospecific interaction is shown to affect the capture efficiency, ϵ, at intermediate range of shear rate G, so that a plateau appears in the curve $\epsilon(G)$, while beyond this range coagulation is governed by Van der Waals attraction and ϵ is a decreasing function of G. This type of dependence is in qualitative agreement with that observed for blood platelet aggregation. Quantitative agreement is achieved with reasonable choice of parameters of interaction. Our approach also makes it possible to take into account the perturbation of particles' trajectories and the corrections to the force of Van der Waals and biospecific interactions due to elastic deformation of particles, which is shown to increase the capture efficiency at low shear rates and decrease it at high shear rates.

1. INTRODUCTION

The problem of coagulation in flowing dispersions is one of the fundamental problems in physics, in colloid chemistry, and especially in biology. The adhesion of biological cells to other cells or to surfaces, including biomaterials, in a fluid stream plays an important role in many biological processes. For example, lymphocyte "homing" during the immune response (1) and tumor metastasis (2) depend on selective adhesion of endothelian cells to blood vessel walls. Biotechnology-related examples include microbial adhesion and certain biological cell separation techniques, such as cell affinity chromatography (3) and endothelian cell seeding of prosthetic vascular grafts (4). Cell–cell and cell–surface interaction can be attributed to the action of colloid and biochemically specific (through receptor–coreceptor bonds) forces (5). The problem of coagulation is especially important for the blood system, primarily as regards thrombus formation (6, 7).

Many of these processes involve collision or very close relative motion between two interacting particles or between particle and substrate, such as the collagen base of a blood vessel or the surface of a filter fibre. A detailed analysis of this close-contact motion requires consideration of the dynamic shape and separation of the particle surfaces in the vicinity of contact which, in turn, influence the interparticle forces and the hydrodynamic interactions between the particles. On the other hand, the hydrodynamic forces acting upon the nearly touching surfaces can cause the particles to deform, especially in the case of nonrigid biological cells. The solid elastic model is a satisfactory approximation for small cells such as blood platelets. In the activated state they acquire spherical form and possess sufficiently developed cytoskeletal structures (8). Typical values of Young's modulus for biological cells are 10^4–10^6 Pa (9).

Thus, the model of elastic spherical particles interacting via the superposition of colloidal and biospecific forces can be used to represent the coagulation of some biological cells, such as activated blood platelets.

The kinetic analysis of irreversible aggregation was carried out by Smoluchowski (10) in terms of approximate theory

[1] To whom correspondence should be addressed. Present mailing address: Dr. A. A. Potanin, Rheology Group, Faculty of Applied Physics, Twente University, Postbus 217, 7500 AE Enschede, The Netherlands.

0021-9797/93 $5.00

which implied that particles and aggregates are moving along straight trajectories up to the moment of their contact. In recent years understanding of the irreversible aggregation of colloids has been enhanced by advances in fluid mechanics. Analyses were mostly restricted to binary coagulation of spherical particles in the shear flow. In this case the probability of a particle being captured by the given particle in unit time is given by

$$J = \tfrac{32}{3}\epsilon a^3 G n, \qquad [1]$$

where G is the shear rate, n is the number of particles per unit volume, a is the particle radius, and ϵ is the so called capture efficiency ($\epsilon = 1$ for Smoluchowski's approximation). Van de Ven and Mason (11) and Zeichner and Schowalter (12) have independently carried out numerical trajectory analyses for the study of colloid stability in flow fields. Two-sphere hydrodynamics and the effect of Van der Waals attraction and electrostatic repulsion were incorporated to predict both rapid coagulation kinetics and the conditions necessary for stability of colloids. The following equation for capture efficiency was obtained (11),

$$\epsilon = c_1 C_A^k, \quad C_A = A/36\pi\eta G a^3, \qquad [2]$$

where η is the medium viscosity, A is the Hamaker coefficient, $c_1 = 1$ and $k = 0.18$ are the coefficients found from the numerical solutions in Ref. (11) or $c_1 = 1.8$ and $k = 0.23$ from Ref. (12). Equation [2] is valid for the system in which the only relevant nonhydrodynamic force is Van der Waals molecular attraction. Recently, an analytical method based on lubrication theory was developed to calculate ϵ for such systems (13).

Application of these theoretical concepts to the description of the coagulation of biological cells requires special analyses of the biospecific interactions of the cells. These interactions involve receptor–coreceptor bonds which are formed between cells during the time of their contact. The numerical simulations of initial stages of biological cells aggregation were carried out by Verkhusha *et al.* (14). Possible secondary doublet formation at very high shear rates due to biospecific receptor–coreceptor interactions between cells was examined. It has been shown that the capture efficiency ϵ of the cells interacting via the biospecific forces is characterized by a weak dependence upon shear rate G up to some critical value, at which ϵ abruptly decreases; i.e., coagulation is to a certain extent suppressed.

Another important specific feature of cells interaction in shear flow concerns their possible deformation. The effect of deformation on the coagulation of particles in shear flow has not been considered up to now. For inertial head-on collision of two elastically deformable spherical particles in a viscous fluid some numerical results for the rebound processes were obtained by Davis and co-workers (15, 16).

In this paper an approximate analytical method incorporating fluid dynamics and elastic solid mechanics is developed for determination of capture efficiency for elastic equal spheres in shear flow. In Section 2 coagulation of rigid spherical particles is considered. Previous analyses are extended in Section 3 by taking into account biospecific receptor–coreceptor interaction of particles, which is relevant to the biological cells (5, 14). Capture efficiency in this case is also calculated. In Section 4 the effect of particle deformation on the shear-induced coagulation will be taken into account. It is shown that this effect can be significant for soft particles, such as biological cells. At last, in Section 5 we briefly describe our experimental data on the aggregation of blood platelets in Couette flow and compare them with the calculations in the framework of our approximate theory.

2. CAPTURE EFFICIENCY FOR RIGID PARTICLES INTERACTING VIA MOLECULAR ATTRACTION

In this section, flow-induced coagulation of rigid particles will be considered in frames of a simplified collision model proposed in Ref. (13). We consider the collision of particles interacting via Van der Waals attraction, which is the most general and best studied case, so that we can compare our calculations with the results of other research.

Let us first assume that the Van der Waals molecular attraction is the sole contributor to colloidal forces between particles. Under conditions of no retardation and small separation gap (gap width $h \ll a$) the force of attraction is given by

$$F_{\mathrm{vdw}}(\xi) = -\frac{Aa}{12h^2} = -\frac{A}{12a\xi^2}, \qquad [3]$$

where $\xi \equiv h/a$ is the dimensionless gap width. According to the model proposed in Ref. (13) the trajectories of particles are calculated without taking into account any kind of interaction except the hydrodynamic one, the later being considered in the framework of the lubrication theory (i.e., it is supposed to be essential only at $\xi \to 0$). Provided the trajectories are calculated, we compare the force of attraction, F_{vdw}, and the hydrodynamic force which stretches the doublet, F_{h}, to formulate the capture criterion in the form $F_{\mathrm{vdw}} + F_{\mathrm{h}} < 0$. Here we briefly consider the basic ideas of this approach and modify it so that it can be utilized in our further analysis.

The velocity $\underline{\mathbf{u}}$ of particle 2 in the coordinate system with origin at the center of particle 1 is given by (16)

$$\underline{\mathbf{u}} = \underline{\mathbf{U}} - \left((A - B)\frac{(\underline{\mathbf{r}} \cdot \underline{\underline{\mathbf{E}}} \cdot \underline{\mathbf{r}})\underline{\mathbf{r}}}{r^2} + B\underline{\underline{\mathbf{E}}} \cdot \underline{\mathbf{r}}\right), \qquad [4]$$

where $\underline{\mathbf{r}}$ denotes the coordinates of particle 2, $\underline{\mathbf{U}} = \underline{\underline{\mathbf{E}}} \cdot \underline{\mathbf{r}} + \underline{\Omega} \times \underline{\mathbf{r}}$ is the unperturbed liquid velocity at $r \to \infty$ for the flow,

which is characterized by the rate of strain tensor $\underline{\mathbf{E}}$ and the angular solid-like rotation $\underline{\Omega}$, and A and B are functions of r. In the framework of the lubrication theory we have

$$A = 1 - \alpha\xi, \quad B = \beta\left(1 + \frac{\lambda}{\ln \xi}\right),$$
$$\alpha = 4.08, \quad \beta = 0.41, \quad \lambda = 1.92. \quad [5]$$

For the simple shear flow in cartesian coordinates we have

$$\underline{\mathbf{U}} = (Gy, 0, 0), \quad \underline{\mathbf{E}} = \frac{1}{2}\begin{pmatrix} 0 & G & 0 \\ G & 0 & 0 \\ 0 & 0 & 0 \end{pmatrix},$$
$$\underline{\Omega} = \left(0, 0, -\frac{G}{2}\right). \quad [6]$$

Spherical coordinates are also used:

$$x = r\cos\theta, \quad y = r\sin\theta\cos\phi, \quad z = r\sin\theta\sin\phi. \quad [7]$$

A sketch of two particles interacting in shear flow, showing the definitions of variables and the coordinate system is given in Fig. 1. As shown in Ref. (13), the following equation can be used to calculate the dimensionless separation gap width ξ_t for the given trajectory,

$$\xi_t = \left(\xi_1^{\Delta} K[\xi_t]\left(\frac{W_0}{2a}\right)^2 + \xi_{\min}^{\Delta}\right)^{1/\Delta} (\cos\theta_0)^{-2/\Delta}, \quad [8]$$

where $\theta_0 \equiv \pi/2 - \theta$ is the angle between $\underline{\mathbf{r}}$ and (y, z)-plane, $K[\xi_t] \equiv (\ln(1/\xi_t)/\ln(1/\xi_1))^{\beta\lambda/\alpha}$, $\Delta \equiv (1 - \beta)/\alpha = 0.15$, ξ_1 is the ξ value which corresponds to the beginning of essential hydrodynamic interaction and is determined according to the equation $B(\xi_1) = 0$, i.e., $\xi_1 = e^{-\lambda} \approx 0.15$, $W_0 \equiv (y_0 + z_0)^{1/2}$, y_0 and z_0 are the coordinates of particle 2 at $r \to \infty$, and

$$\xi_{\min} \equiv (\beta J/2\alpha)^{1/\Delta}, \quad J \equiv \frac{\xi_1^{\Delta}}{\Delta} + \lambda Ei(\Delta \ln(\xi_1)). \quad [9]$$

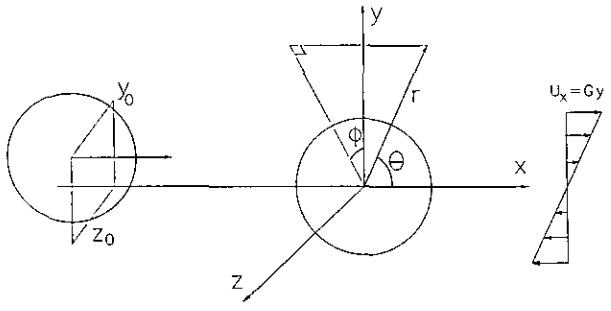

FIG. 1. Schematic of the collision of particles in shear flow.

Equation [8] can be solved numerically to determine $\xi_t(\theta_0)$ at different W_0 values. Here we need to know the limiting value $\xi_t(\theta_0 \to 0)$ to formulate the capture criterion. According to the lubrication model, the given pair of particles is moving like a free doublet and the radial component of the hydrodynamic stretching force is given by (17)

$$F_{str}(\theta_0, \phi) = 2P(r \to 2a)\eta a^2 G \sin 2\theta_0 \cos\phi, \quad [10]$$

where $P(r)$ is some function of the distance between centers of spheres such that $P(r \to 2a) = P_0 = 3.1\pi$. A capture criterion can now be written in the form

$$F_{Vdw}(\xi_c) < F_{str}(\theta_c, \phi) \equiv 2P_0\eta a G^2 \sin 2\theta_c \cos\phi. \quad [11]$$

where ξ_c and θ_c are the values of ξ_t and θ_0 such that at $\theta_0 < \theta_c$ or $\xi_t < \xi_c$, Van der Waals attraction dominates hydrodynamic stretching. Equation [11] is relevant for the closest section of the trajectory, implying $\theta_c \ll 1$. Combining [8] and [11] we write the capture criterion in the form

$$\xi_t(\theta_0 \to \theta_c) < \xi_c(\phi) \equiv \left(\frac{0.48C_A}{\sin 2\theta_c \cos\phi}\right)^{1/2}. \quad [12]$$

This criterion should be considered semiphenomenological, because it includes the parameter θ_c which is not calculated in the framework of this approach. This parameter characterizes the captured section of the trajectory (i.e., the section of the trajectory along which the particles are moving as a joined doublet). Estimation of θ_c are given below on the basis of comparison with the numerical calculations. Making use of [8] and [12] we find an equation for the capture cross section:

$$W_0(\phi)/2a = \left\{\frac{1}{\xi_1^{\Delta} K[\xi_c(\phi)]}(\cos^2\theta_c \xi_c^{\Delta}(\phi) - \xi_{\min}^{\Delta})\right\}^{1/2}. \quad [13]$$

The collision frequency is given by

$$J = 4nGa^3 \int_0^{\pi/2} d\phi' \int_0^{W_0(\phi')/a} dr r^2 \cos\phi'. \quad [14]$$

Here ϕ' is the value of ϕ which characterizes the particles relative position at infinite separation ($r \to \infty$, $\theta_0 \to -\pi/2$). In frames of our approximate analysis ϕ' is identified with ϕ. It can be easily shown that the corrections which arise when the difference between ϕ' and ϕ is taken into account are small. If $W_0 = 2a$ (no hydrodynamic interaction) we would obtain the Smoluchovski formula [1] with $\epsilon = 1$. According to Eq. [14] capture efficiency for interacting particles is given by

$$\epsilon = \int_0^{\pi/2} (W_0/2a)^3 \cos\phi \, d\phi. \qquad [15]$$

Substituting [13] into [15] and calculating numerically the integral in [15] one finds the capture efficiency ϵ as a function of shear rate G or dimensionless group C_A. It should be noted that in Ref. (13) an additional simplifying assumption was utilized which implies that in Eq. [8] one should put $K[\xi_t] \to K[\xi_{min}]$. In this case an analytical estimate for the capture efficiency can be found as $\epsilon(C_A) = 0.7C_A^{0.11}$. However, this equation overestimates ϵ, so we use a more precise approach here, which turns out to be in good agreement with numerical calculations.

Comparison of the calculations according to our simplified model and numerical results of Van de Ven and Mason (11) and Zeichner and Schowalter (12) is presented in Fig. 2. There is a certain discrepancy between (11) and (12) at low shear rate due to different integration procedures used in these works. As pointed out above, our semiphenomenological theory includes one fitting parameter, θ_c, which should be chosen to best fit the numerical data. The best agreement with (11) was achieved at $\theta_c \geqslant 0.1$, while the best agreement with (12) at $\theta_c \leqslant 0.15$. To discuss the difference between (11) and (12) is beyond the scope of the present work. In frames of our simplified approach it is sufficient to set θ_c equal to some intermediate value, say $\theta_c = 0.125$, which guarantees that the error of calculations does not exceed 20%. This value is used below.

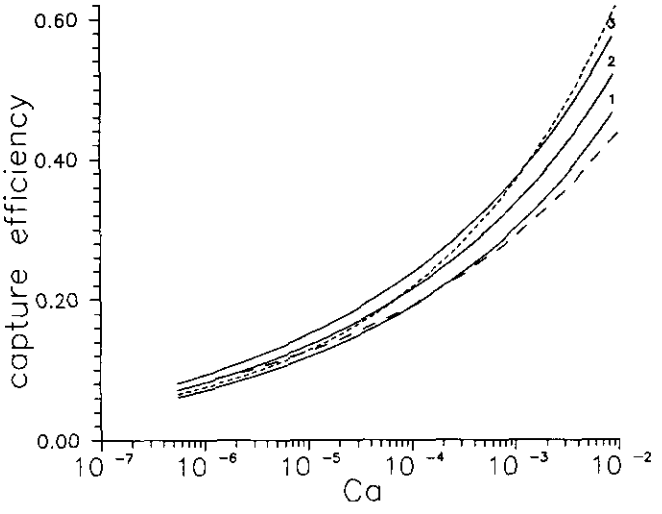

FIG. 2. Capture efficiency is plotted against C_A for rigid particles interacting via molecular attraction. Curves 1–3 are calculated numerically according to Eqs. [12], [13], and [15], with $\theta_c = 0.10$ (1), 0.125 (2), 0.15 (3). Dashed curve corresponds to the analysis of Ref. (11) based on the numerical calculations of trajectories; dotted curve to Ref. (12).

3. PARAMETERS OF SPECIFIC INTERACTION OF BIOLOGICAL CELLS AND CAPTURE EFFICIENCY CALCULATIONS IN SHEAR FLOW

In this section cell–cell adhesion in the shear flow is considered to result from the interplay of two subsystems, the chemical and mechanical ones. Receptors (R) and their specific coreceptors (L) located on the surface of the cells comprise the chemical subsystem. On cell collision, R and L, located on different cells, form a specific complex RL that binds the cells together. (See Fig. 3.) Interaction between R and L located on the same cell is considered impossible. The mechanical subsystem is represented by the shear flow which brings the cells together to the distance at which the formation of intercellular bonds is possible. If the number of bonds formed during the interaction time is insufficient the flow carries the cells away from each other.

The biospecific component of the force arises from the formation of intercellular adhesive bonds RL. This process can be subdivided into two stages (18, 19). The first stage involves the approach of the reacting pair to a position (the formation of the so-called encounter complex, R · · · L) in which the distance between molecules and their orientation allows the second stage (the chemical reaction itself) to proceed (20–23). Exact analysis of the receptor and coreceptor diffusion should be carried out, taking into account both the orientation and translation movement of the mass centers of reacting molecules. To simplify the analyses let us first of all point out that the orientational process is more rapid than the translational one (22), so that the first stage can be described in terms of translational diffusion alone.

The lateral diffusion coefficients, D, of various protein molecules in cell membranes, including receptors, have been measured by the fluorescence photobleaching recovery technique (24, 25). They range between the limits 10^{-12}–10^{-15} m^2/s. It is interesting to compare these values with those calculated according to the Einstein equation, $D = kT/\mu$, where the friction coefficient can be written as $\mu = 6\pi C_f \eta c$, c is effective radius of the receptor, and C_f is the coefficient which is introduced to take into account the high friction force imposed on the receptor moving in the membrane ($C_f = 1$ for the Stokesean friction). Assuming $c \sim 10$ nm, $\eta \sim 1$ mPa · s, one can see that the measured values of D correspond to $C_f \sim 20$–2×10^4; i.e., the true friction is higher than the Stokesean friction. To understand this phenomena one can utilize the model (26–28), according to which the protein molecule is represented by a cylindrical disc of radius c moving in the cell membrane which is represented by a two-dimensional layer of continuous fluid of viscosity η_m. The thickness of the disc is equal to the thickness of the membrane, l_m, while the viscosity of the membrane, η_m, is several orders of magnitude larger than the viscosity of intercellular fluid. Calculations carried out in Refs. (26, 27) yielded an estimate of D valid at $\eta_m l_m/(\eta c) \gg 1$. In this case C_f can be estimated as

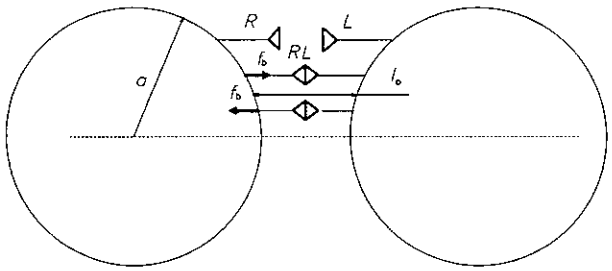

FIG. 3. Schematic of the contact zone of two cells connected by receptor–coreceptor bonds.

$$C_f \sim \frac{2}{3}\frac{\eta_m}{\eta}\frac{1}{\ln[\eta_m l_m/(\eta c)] - 0.5772}. \qquad [16]$$

Typically $\eta_m \sim 10^2\eta_0$, $l_m \sim c$, so that $C_f \approx 20$, which corresponds to the lower bound of the interval quoted above. Higher values of C_f are usually attributed to the effects of cytoskeleton or other objects inside the cell, which the protein can be attached to, or phase transitions in the membrane (28).

The two-stage interaction of receptors and coreceptors is described by the kinetic scheme

$$R_{1.2} + L_{2.1} \underset{k_2}{\overset{k_1}{\rightleftarrows}} R_{1.2}\cdots L_{2.1} \underset{k_4}{\overset{k_3}{\rightleftarrows}} R_{1.2}L_{2.1}, \qquad [17]$$

where k_1 and k_2 are diffusion rate constants for the formation and breakup of R · · · L, respectively, and k_3 and k_4 are intrinsic rate constants depending on the energy and the mechanism of RL formation and breakup. Subscripts 1 and 2 denote two distinct cells.

Let us obtain estimates for k_1 and k_2. Assume for simplicity that the cell membranes in the region of contact (that is, in the region where the surface molecules of one cell are accessible for the reacting molecules of the other) are locally planar. The process of formation and breakup of encounter complexes, R · · · L, can be described as the two-dimensional aggregation of receptors and coreceptors located on the opposite surfaces of interacting cells. Relative movement of receptors and coreceptors is a superposition of the local relative movement of the surfaces of the cells in the vicinity of their contact, $V_{loc}(\theta, \phi)$, and the Brownian movement of receptors and coreceptors, which is characterized by diffusion coefficients D_r and D_l, respectively. Below we assume for simplicity that the diffusion coefficients, D_r and D_l, and effective radii, c_r and c_l, of receptors and coreceptors are equal: $D_r = D_l = D$, $c_r = c_l = c$. The number of encounter complexes formed per unit time per unit surface due to the aggregation between receptors and coreceptors can be estimated as

$$k_1[R][L] = (k_{1b}D + 2cV_{loc})[R][L], \qquad [18]$$

where [R] and [L] are the surface concentrations of receptors and coreceptors on the two respective cells, and k_{1b} is a numerical coefficient.

The rate constant for R · · · L breakup is the reciprocal of the mean time of R and L relative shift to a distance equal to the sum of characteristic dimensions of the targets, $c_R + c_L = 2c$. Making use of the estimate of this time obtained for the case of two-dimensional diffusion (22, 23, 29) and adding the contribution due to the relative movement of the surfaces one finds the expression for the number of broken R · · · L complexes per unit time per unit surface

$$k_2[R\cdots L] = \left(k_{2b}\frac{D}{c^2} + \frac{V_{loc}}{2c}\right)[R\cdots L], \qquad [19]$$

where k_{2b} is a numerical coefficient.

The estimations of k_{1b} and k_{2b} require more accurate analysis of two-dimensional Brownian movement of protein molecules and their aggregation–disaggregation process. As shown in Refs. (22, 29), $k_{2b} \sim 1$ is a constant, while $k_{1b} < 1$ is a logarithmic function of c and surface concentrations of proteins. Below we see that for the typical range of shear rates in which biospecific interactions are relevant to the coagulation of cells, one can assume $V_{loc} \gg cD$, so that in Eqs. [18, 19] second terms in the brackets dominates. Hence k_1 and k_2 are constant.

Now let us consider the intrinsic rate constants k_3 and k_4. Let l_0 denote the width of the gap between the membranes at the steady configuration of the membrane-RL-membrane complex. Any gap width l (e.g., $l > l_0$) can be associated with an excess energy of the complex, $\phi(l)$. In the liner-elastic approximation (30–32) $\phi(l)$ is given by

$$\phi(l) = \phi(l_0) + \tfrac{1}{2}\delta(l - l_0)^2. \qquad [20]$$

In the general case, the stiffness coefficient, δ, is determined by the stiffness of the most flexible link of the complex. In the model of rigid cells under consideration this can be either the bonding regions in the active sites or fragments of R and L devoid of secondary structure. The upper bound of δ is apparently the stiffness of alpha-helical protein segments, $\delta = 1$ N/m (33). The elastic force f_b exerted on the cell doublet by a single intercellular bond is given by

$$f_b = -\frac{\partial\psi(l)}{\partial l} = -\delta(l - l_0). \qquad [21]$$

The influence of the intermembrane distance on the chemical reaction between R and L is obvious from Eq. [20]. We suppose the bond to be broken if the elastic energy per bond exceeds some activation energy of the bond U_a, i.e.,

$$k_3 = k_{30},\ k_4 = k_{40}, \quad \text{at } |l - l_0| < (2U_a/\delta)^{1/2}, \qquad [22.1]$$

$$k_3 = 0,\ 1/k_4 = 0, \quad \text{at } |l - l_0| > (2U_a/\delta)^{1/2}. \qquad [22.2]$$

Below for simplicity the index "0" in k_{30} and k_{40} is omitted. For U_a we take a typical value $U_a \sim 10kT$. It should be noted that Eqs. [22] give the simplest representation for the dependences of k_3 and k_4 upon the elongation of the bond, $l - l_0$. There are more accurate approaches based on the conditions of detailed balance which yield exponential dependences of k_3 and k_4 upon $l - l_0$ (14). However, it is easy to show that the resultant equation for the force of biospecific interaction is very similar in both cases; i.e., the precise form of the dependence of k_3 and k_4 upon $l - l_0$ is not very important in the first approximation. Let us now discuss possible estimates for k_3 and k_4 available from the literature. Pecht and Lancet (35) give values 10^6–10^9 s^{-1} and 10^{-3}–10^3 s^{-1}, respectively, for various hapten–antibody interactions. Bell (18) reports the values of $k_3 \sim 10^5$ s^{-1} for the binding of concanavalin A with the erythrocytic membrane and $k_4 \sim 10^2$ s^{-1} for a typical antigen–antibody reaction. Studies on the adhesive interactions of cytotoxic T-cell clone F1 with its target cell clone JY as well as of the T-cells with each other yield k_4/k_3 estimates of 1 and 10^{-2}, respectively (36). Abbott and Nelsestuen used a value of $k_4/k_3 \sim 10^{-9}$ when modeling ligand binding to membrane-bound receptors on small cells (37). Wiley, in his model of membrane protein turnover, used values of 10^{-4} to 10^{-2} s^{-1} for k_4 in the case of a typical receptor (38). Despite a considerable spread of these data it seems reasonable to assume in most cases that $k_3 > k_4$ and $k_3 \geqslant 10^6$ s^{-1}. This is sufficient for our further analysis.

The force of biospecific interaction of two spherical cells can be related to the force of interaction per unit area of plane membranes, $\Pi_s(H)$, separated by the gap H, according to the well known Derjaguin approach (39):

$$F_s = \pi a \int_h^\infty \Pi_s(H) dH. \qquad [23]$$

Equation [23] is valid if the interaction occurs at gap widths much smaller than a, i.e., $l_0 \ll a$. Our next purpose is to calculate $\Pi_s(H)$. According to Eqs. [22] receptor–coreceptor bonds are assumed to exist in the region which is defined by the condition $|H/a - \xi_0| < \Delta \equiv (2U_a/(\delta a^2))^{1/2}$ so that we can write

$$\Pi_s(H) = -[RL] a\delta\left(\frac{H}{a} - \xi_0\right) Q\left(\Delta - \left|\frac{H}{a} - \xi_0\right|\right), \qquad [24]$$

where $Q(x)$ is a step function defined so that $Q(x) = 1$ if $x > 0$ and $Q(x) = 0$ if $x > 0$. Thus, according to our model, two surfaces interact only if the distance between them belong to the final interval defined by Eq. [24]. Hence, the contribution into the integral [23] is given only by some *active zone*, i.e., a part of the surface which exists only if $\xi_0 + \Delta < \xi$ and has a form of a ring (if $\xi < \xi_0 - \Delta$) or a circle (if $\xi_0 + \Delta > \xi > \xi_0 - \Delta$).

As distinct from most forces traditionally considered in colloid chemistry, the force of interaction Π_{spec} is nonstationary. To demonstrate this let us consider the interaction of two surfaces which were put together in the moment $t = 0$ and stayed in contact, being separated by the gap H, such that $|H/a - \xi_0| < \Delta$. The concentration of adhesive bonds, [RL], can be found by solving the system of kinetic equations

$$\frac{\partial[R\cdots L]}{\partial t} = 2k_1[R][L] - (k_2 + k_3)[R\cdots L] + k_4[RL], \qquad [25.1]$$

$$\frac{\partial[RL]}{\partial t} = k_3[R\cdots L] - k_4[RL], \qquad [25.2]$$

with the initial conditions

$$[R](t = 0) = [R]_0, \quad [R\cdots L](t = 0) = 0, \qquad [26.1]$$

$$[L](t = 0) = [L]_0, \quad [RL](t = 0) = 0. \qquad [26.2]$$

Conservation laws for R and L on both cells' surfaces are satisfied:

$$[R]_0 = [R] + [R\cdots L]/2 + [RL]/2, \qquad [27.1]$$

$$[L]_0 = [L] + [R\cdots L]/2 + [RL]/2. \qquad [27.2]$$

The solution of Eqs. [25] can easily be found if we assume that $k_2 \ll k_3$. By making use of [19] and taking into account that $V_{loc} \sim aG$, $k_3 \geqslant 10^6$ s^{-1}, $c \sim 10$ nm, $a \sim 1$ μm, we find that this assumption holds true for $D \ll 10^{-10}$ m^2/s, $G \ll 10^4$ s^{-1}. Both of these inequalities are usually satisfied. Now we write down the solution of Eqs. [25]–[27] in two cases. For $[R]_0 = [L]_0$ we find

$$[RL] = 2[R]_0 \frac{k_3}{k_3 + k_4}(1 - \exp[-(k_3 + k_4)t]) - 2\frac{k_3}{k_1}\exp\left(-\frac{k_3 + k_4}{k_1[R]_0} - (k_3 + k_4)t\right) \times \left\{Ei\left(\frac{k_3 + k_4}{k_1[R]_0} + (k_3 + k_4)t\right) - Ei\left(\frac{k_3 + k_4}{k_1[R]_0}\right)\right\}, \qquad [28]$$

where $Ei(x) = \int_{-\infty}^{x} \exp(x')dx'/x'$. For $[L]_0 \ll [R]_0$ we have

$$[RL] = 2[L]_0\left(\frac{k_3}{k_3 + k_4} + \frac{k_3\exp(-k_1[R]_0 t)}{k_1[R]_0 - (k_3 + k_4)} - \frac{k_1 k_3 [R]_0 \exp[-(k_3 + k_4)t]}{(k_3 + k_4)(k_1[R]_0 - k_3 - k_4)}\right). \qquad [29]$$

The experimental data considered in Section 5 correspond to the later case. From Eq. [29] one can see that the stationary solution in this case is given by

$$[\mathrm{RL}](t \to \infty) \equiv 2[\mathrm{L}]_0 \frac{k_3}{k_3 + k_4} \approx 2[\mathrm{L}]_0 \qquad [30]$$

and is valid at

$$t \gg \max\{1/(k_1[\mathrm{R}]_0),\ 1/(k_3 + k_4)\}. \qquad [31]$$

In shear flow the time of a contact t can be estimated as $t \sim 1/G$. Those cases, in which stationary solution [30] can be applied, permit a simple calculation of the force F_{spec}. This holds true for the systems considered below. Substituting [30] into [24] and [24] into [23] we find

$$F_s = -2\pi a[\mathrm{L}]_0 U_a \left(1 - \frac{(\xi - \xi_0)^2}{\Delta^2}\right) Q(\Delta - |\xi - \xi_0|). \qquad [32]$$

Thus, in this case the force of biospecific interaction of spherical surfaces is purely attractive and nonzero only if the distance between surfaces is close enough to the critical value ξ_0.

Assuming the force of biospecific interaction to be given by the stationary limit [32] we can now formulate the capture criterion by generalizing [11] as

$$-F_{\mathrm{VdW}}(\xi_c) - F_s(\xi_c) < F_{\mathrm{str}}(\theta_c, \phi). \qquad [33]$$

Making use of the criterion [33] we find an equation which determines ξ_c as a function of ϕ (analogue of the criterion [12]),

$$\frac{0.48 C_A}{\xi_c^2(\phi)} + C_B Q(\Delta - |\xi_0 - \xi_c(\phi)|) = \sin 2\theta_c \cos\phi, \qquad [34]$$

where $C_B \equiv F_s(\xi_c(\phi))/(2P_0\eta_0 a^2 G)$. If there is no biospecific component of interaction, i.e., $C_B = 0$, Eq. [34] is equivalent to criterion [12]. If $C_B > 0$, Eq. [34] can be solved numerically. Substituting $\xi_c(\phi)$ into Eq. [13], one finds $W_0(\phi)$. After that the capture efficiency is calculated according to Eq. [15].

Here it is important to point out that Eq. [34] implies that the trajectories of particles are identical to those of non-touching spheres. However, the ligand–receptor bonds between surfaces can prevent the particles from free rotation so that the doublet should be rather represented by a rigidly connected dumbbell, i.e., secondary doublets can turn into primary ones, according to the terminology of Van de Ven and Mason (40). This transition does not occur if the friction coefficient of the protein molecule, μ, or the dimensionless coefficient, C_f, is low enough. It is useful to write down the condition which guarantees that such transition does not occur so that the doublet can be described as secondary during its rotation. To do this we compare the external hydrodynamic torque applied to the sphere by the flow, $T_{\mathrm{hyd}} \sim \eta G a^3$, and the torque resisting its rotation, which arises due to bonds between the surfaces, $T_{\mathrm{bond}} \sim \mu V_{\mathrm{loc}} a[\mathrm{L}]_0 A_{\mathrm{con}}$, where A_{con} is the area of the active zone on the surface of the particle. According to [24] the active zone is determined by the inequality $\Delta > |H/a - \xi_0|$, where H in the vicinity of contact is approximated by a paraboloid, $H/a = \xi + (r/a)^2$, so that at $\xi \to \xi_0$ we have $A_{\mathrm{con}} \sim \Delta a^2$. Now the inequality $T_{\mathrm{hyd}} \gg T_{\mathrm{bond}}$ takes the form

$$1 \gg C_f[\mathrm{L}]_0 U_a/\delta. \qquad [35]$$

Results of the calculations of the capture efficiency are plotted in Figs. 4–8. In Figs. 5–8 calculated curves are compared with the experimental data discussed in Section 5. One can see that the biospecific interaction affects the coagulation at intermediate shear rates increasing the capture efficiency, so that a "plateau" appears in the curve $\epsilon(G)$. The existence of the plateau at intermediate shear rate is confirmed by experimental measurements of the coagulation rate of the platelets. The range of shear rate at which the plateau appears turns out to be the most important for the dynamics of thrombous formation.

Let us check the applicability of the assumptions [31] and [35] in the range of shear rate which correspond to the intermediate shear rate plateau of the curve, $G \sim 10^2$–$10^3\ \mathrm{s}^{-1}$. Typical parameters of the system are $a = 1\ \mu\mathrm{m}$, $c = 10$ nm,

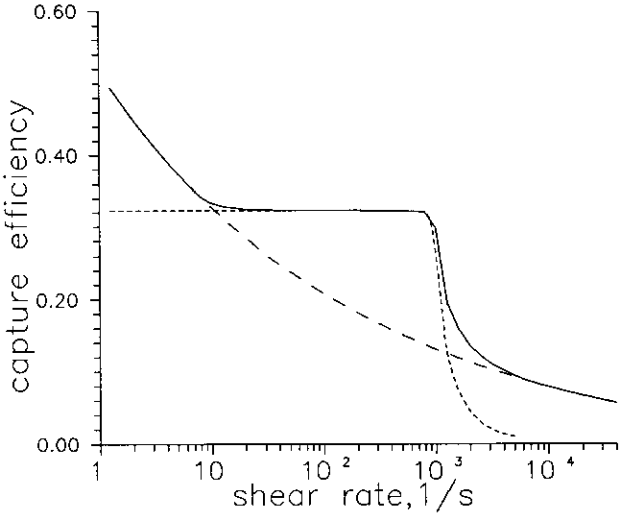

FIG. 4. Capture efficiency for rigid particles is plotted vs shear rate. Dashed curve corresponds to particles interacting via molecular attraction; dotted curve corresponds to particles with biospecific interactions; solid curve corresponds to particles interacting via superposition of molecular attraction and biospecific interaction. The values of parameters are typical for small biological cells (5, 17, 29, 33): $a = 1\ \mu\mathrm{m}$, $A = 10^{-21}$ J, $\eta_0 = 1$ mPa·s, $\tau c^2[\mathrm{L}]_0 = 0.02$, $c = 10^{-8}$ m, $\delta = 10^{-2}$ N/m, $\xi_0 = 0.03$.

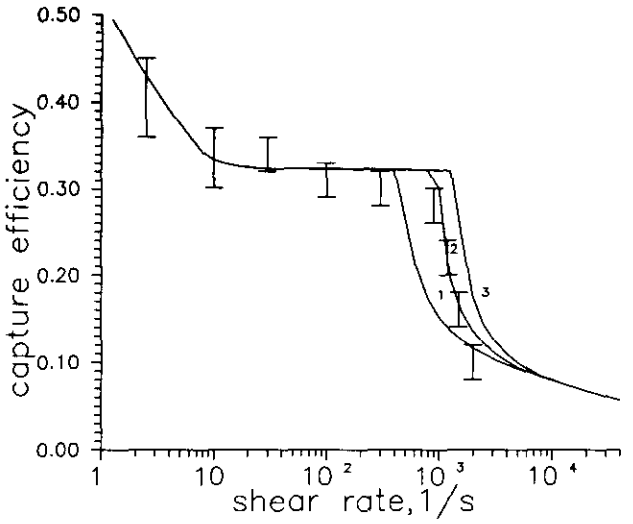

FIG. 5. Capture efficiency for particles interacting via superposition of molecular attraction and biospecific interaction is plotted vs shear rate at $\pi c^2[L]_0 = 0.01$ (1), 0.02 (2), 0.03 (3). Other parameters are the same as in Fig. 4.

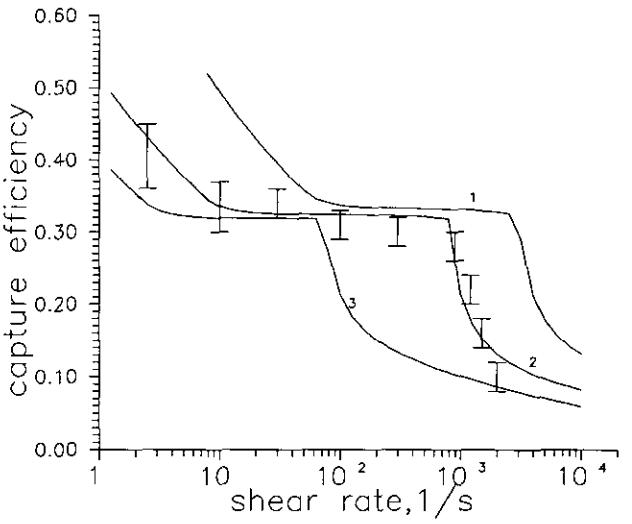

FIG. 7. Capture efficiency for particles interacting via superposition of molecular attraction and biospecific interaction is plotted vs shear rate at a (μm) = 0.5 (1), 1.0 (2), 1.5 (3). Other parameters are the same as in Fig. 4.

$U_a = 10$ kT, $\delta = 0.01$ N/m, $[R]_0 \gg [L]_0 \sim 0.01/c^2$, $k_4 < k_3 = 10^6$ s^{-1}. In this case the right-hand side of [31] can be written as $1/(Gac[R]_0)$, so that the stationary solution is applicable if $[R]_0 \gg 0.01/c^2$. Calculating the right-hand side of [35] we find that $C_f \ll 10^3$. One can see that our approach is valid if the surface concentration of receptors is not very low and the friction coefficient is not very high.

4. EFFECT OF PARTICLE DEFORMATION ON THE COAGULATION

In this section we calculate the capture efficiency of particles, taking into account their deformation due to the hydrodynamic pressure in the gap between their surfaces. Our consideration is carried out in the framework of the same lubrication theory approach, as was used above for calculating the capture efficiency of rigid particles. Our objective now is to calculate the perturbation of the shape of the particle surfaces, assuming this perturbation to be small. After that we calculate the perturbation in the capture efficiency arising from the deformation. In our calculations we consider the cell to be a solid elastic particle. This is a satisfactory approximation for small cells, for instance blood platelets with spreading bulk cytoskeletal structures (8).

The area of contact of two elastic spheres is shown in Fig.

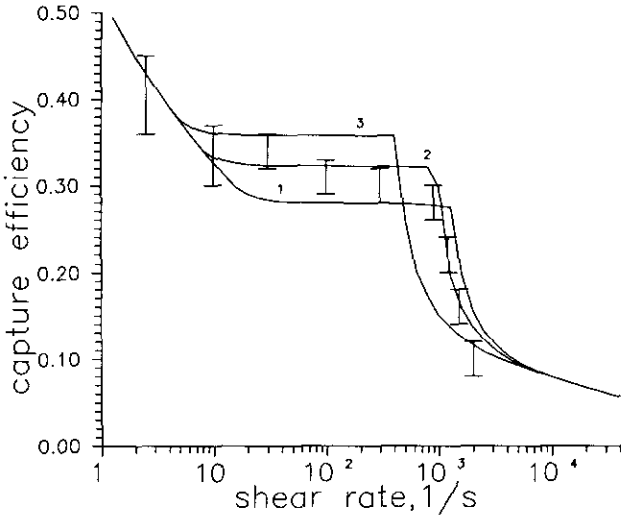

FIG. 6. Capture efficiency for particles interacting via superposition of molecular attraction and biospecific interaction is plotted vs shear rate at ξ_0 = 0.01 (1), 0.03 (2), 0.05 (3). Other parameters are the same as in Fig. 4.

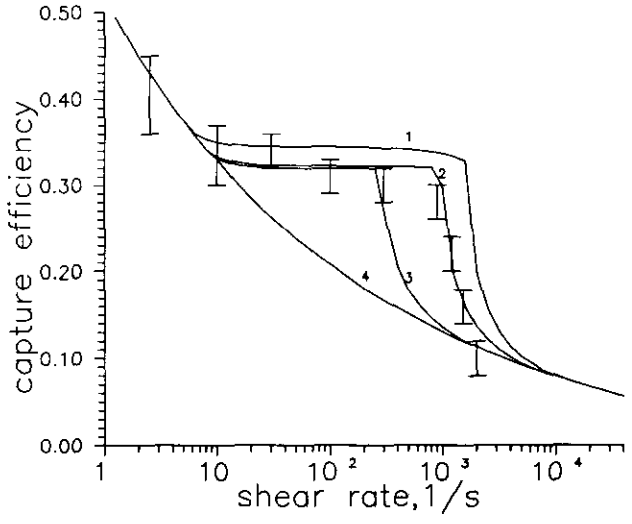

FIG. 8. Capture efficiency for particles interacting via superposition of molecular attraction and biospecific interaction is plotted vs shear rate at δ (N/m) = 0.001 (1), 0.01 (2), 0.02 (3), 0.03 (4). Other parameters are the same as in Fig. 4.

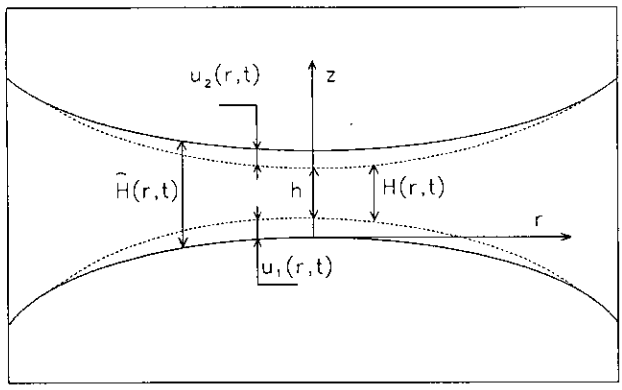

FIG. 9. Schematic of the contact zone of two deformable particles. Dashed line, undeformed surfaces; solid line, deformed surfaces.

9. In the framework of the lubrication theory approach the undeformed spherical surfaces are approximated by paraboloids in the region of near contact,

$$H(r, t) = h(t) + r^2/a, \qquad [36]$$

while the perturbed gap profile is given by

$$\tilde{H}(r, t) = H(r, t) + u(r, t), \qquad [37]$$

where $h(t)$ is the distance between the unperturbed surfaces and $u(r, t) = u_1 + u_2$ is the sum of the dynamic deformations of the two surfaces from their original shape due to hydrodynamic pressure. Here and everywhere below the tilde ˜ is used to denote the perturbed values. In order to determine the deformation u we follow the development of the Hertz contact theory of linear elasticity (see, e.g., (41)) and also that of Davis and co-workers (15, 16), who have studied the deformation of particles colliding head-on in liquid.

The analysis of particle capture is carried out in the framework of the simplified model formulated in Section 2, generalizing it to the case of deformable particles; i.e. we calculate the trajectories of particles (including their perturbation due to deformation), neglecting all types of interaction except near-contact (lubrication) hydrodynamics, and assume coagulation to occur when the attractive force on the particles (which also includes a correction due to deformation) exceeds the hydrodynamic force. According to this approach, we start from the elastohydrodynamic problem of calculating the deformation of particles and corresponding corrections to their trajectories.

The deformation of particles arising due to hydrodynamic pressure in the gap between their surfaces, u_h, is given by

$$u_h = 8\frac{1-\nu^2}{\pi E}\int_0^\infty K\left(\frac{2\sqrt{r'r}}{r'+r}\right)\frac{\tilde{p}(r', t)}{r'+r}\,r'dr, \qquad [38]$$

where

$$K(k) = \int_0^{\pi/2}\frac{d\phi}{\sqrt{1-k^2\sin^2\phi}} \qquad [39]$$

is the complete elastic integral of the first kind and $\tilde{p}(r', t)$ is the pressure profile in the fluid layer. It is easy to show that Eq. [39] can be rewritten in the form

$$u_h = -\frac{1-\nu^2}{E}\eta V\xi^{-3/2} f_h(r/\sqrt{ah}), \qquad [40]$$

where the following easily tabulated dimensionless function is introduced:

$$f_h(\zeta) = \frac{12}{\pi}\int_0^\infty K\left(\frac{2\sqrt{\zeta'\zeta}}{\zeta'+\zeta}\right)\frac{\zeta' d\zeta'}{(\zeta'+\zeta)(1+\zeta'^2)^2}. \qquad [41]$$

To calculate $\tilde{p}(r', t)$ one should solve the equation

$$\frac{\partial\tilde{H}}{\partial t} = \frac{1}{12\eta r}\frac{\partial}{\partial r}\left(r\tilde{H}^3\frac{\partial\tilde{p}}{\partial r}\right) \qquad [42]$$

together with the boundary conditions

$$\tilde{p}(r\to\infty) = 0, \quad \partial\tilde{p}(0, t)/\partial r = 0. \qquad [43]$$

To complete the formulation of the basic model, one also needs the kinematic equation, which describes the relative motion of the undeformed surfaces of the solid spheres,

$$\frac{dh}{dt} = V, \qquad [44]$$

where V is the relative velocity of the center of masses of the two spheres.

Eqs. [38], [42], and [44] constitute a self-consistent set of equations which can be solved numerically, as it was done, e.g., in Refs. (15, 16) for inertial motion. However, here we consider an approximate method of solution which is relevant in the limit $u_h \to 0$ or $E \to \infty$ (i.e., one should require the condition $u_h \ll h$ to be obeyed in addition to a usual condition of small deformation $u_h \ll a$). In this case, the unperturbed solution of Eq. [43] can be used, which is given by

$$p(r) = -\frac{3}{2}\eta\frac{Va}{H^2}. \qquad [45]$$

The relative velocity of particles according to the lubrication model is given by

$$V = (1-A)Ga\sin 2\theta_0\cos\phi = \alpha\xi Ga\sin 2\theta_0\cos\phi. \qquad [46]$$

Equations [40], [41], and [46] determine the dynamic deformation of particles. The maximum value of deformation corresponds to the point near contact $r = 0$ (see Fig. 9). The dimensionless maximum dynamic deformation, u_{hmax}, is defined according to the formula

$$u_{\text{hmax}} \equiv u_{\text{h}}(r = 0)\frac{E}{(1 - \nu^2)a\eta G}. \qquad [47]$$

According to Eqs. [45]–[47] we find that

$$u_{\text{hmax}} = -\frac{3}{2}\alpha\pi\xi_{\text{t}}^{-1/2}\sin 2\theta_0\cos\phi, \qquad [48]$$

where ξ_{t} is found from the solution of Eq. [8] provided W_0 is given. In Fig. 10 u_{max} is plotted vs θ_0 at $\phi = 0$. One can see that u_{max} is increased as W_0 is decreased.

As pointed out above, our approach is valid for small deformations, i.e., $u_{\text{h}} \ll h$. Making use of Eqs. [47] and [48] we can write this criterion in the following form:

$$(1 - \nu^2)\frac{\eta G}{E}\xi_{\text{t}}^{-3/2} \ll 1. \qquad [49]$$

Since in our calculations of capture efficiency only critical trajectories are relevant, i.e., $\xi_{\text{t}} \to \xi_{\text{c}}(\phi)$, we substitute into Eq. [49] $\xi_{\text{c}}(\phi)$ instead of ξ_{t}, so that the criterion of applicability of our approach now takes the form

$$(1 - \nu^2)\frac{\eta G}{E}[\xi_{\text{c}}(\phi)]^{-3/2} \ll 1. \qquad [50]$$

In the framework of the lubrication theory the force of the hydrodynamic resistance to the relative movement of two undeformable spherical particles is written as

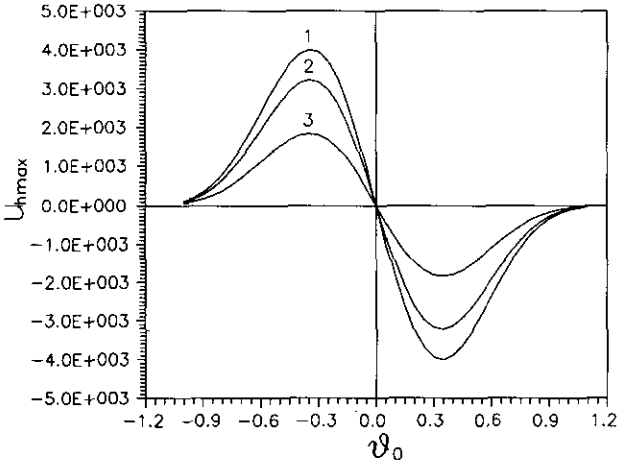

FIG. 10. Maximum dimensionless dynamic deformation u_{hmax} is plotted vs. θ_0 for $W_0/2a \to 0$ (1), $W_0/2a \to 0.1$ (2), $W_0/2a \to 0.2$ (3).

$$F_{\text{h}}(\xi) = 2\pi\int_0^\infty p(r)rdr = \pi a\int_h^\infty p(H)dH = -\frac{3}{2}\pi\eta aV\xi^{-1}, \qquad [51]$$

where we utilized Eq. [36] to change the variable in the integral from r to H. For deformed particles in the limit $u \to 0$ the perturbation of the force due to deformation can be calculated as follows:

$$\tilde{F}_{\text{h}} = F_{\text{h}} + \Delta F_{\text{h}},$$
$$\Delta F_{\text{h}} = \pi a\int_h^\infty \frac{dp(H)}{dH}u_{\text{h}}(\sqrt{a(H - h)})dH. \qquad [52]$$

Making use of [40] and [45] we find that

$$\Delta F_{\text{h}}(\xi) = -C\frac{(\eta V)^2(1 - \nu^2)}{E}\xi^{-7/2}, \qquad [53]$$

where

$$C = 3\pi\int_1^\infty \frac{f_{\text{h}}(\sqrt{\zeta - 1})}{\zeta^3}d\zeta = 16.2. \qquad [54]$$

Equation [53] can be used to calculate the corrections to the trajectories of particles due to the deformation. In the framework of the lubrication model used here it is sufficient to determine the corrections to A or $\alpha \equiv (1 - A)/\xi$. To do so we follow Batchelor and Green (17) and consider particles 1 and 2 with centers on the axis z in the elongation flow defined by the rate of strain tensor $\underline{\mathbf{E}}$ with three nonzero components: $E_x = E_{yy} = -G/2$, $E_{zz} = G$, and $\Omega = 0$. In this case the equation of force balance, $F_{\text{str}} + F_{\text{h}} + \Delta F_{\text{h}} = 0$, and the relative velocity of particles, V, takes the form

$$8P_0\eta a^2G - 3\pi a^2\eta\alpha G + \Delta F_{\text{h}} = 0, \quad V = 2\alpha aG/\xi. \qquad [55]$$

If the particles are rigid, i.e., $\Delta F_{\text{h}} = 0$, Eq. [55] gives the known estimate $\alpha = 8P_0/3\pi = 4.08$ (see Eq. [5]). Now we make use of Eq. [55] to find a correction to α as

$$\tilde{\alpha} = \alpha\left(1 + \frac{\Delta F_{\text{h}}}{3\pi\eta\xi^{-1}a^2G}\right) = \alpha\left(1 + \frac{8P_0\Delta F_{\text{h}}}{9\pi^2\eta\xi^{-1}aV}\right). \qquad [56]$$

Although Eq. [56] was derived for elongation flow, it can be applied as well to any other type of flow provided V is properly defined. For shear flow, V is given by Eq. [46]. Making use of Eqs. [54]–[56], we finally find that

$$\tilde{\alpha} = \alpha\left(1 - 0.86C\frac{(1 - \nu^2)\eta V}{aE}[\xi_{\text{c}}(\phi)]^{-5/2}\right), \qquad [57]$$

where we substituted $\xi \to \xi_c(\phi)$, as corresponds to our capture criterion. Corrections to Δ are calculated in accordance with [57]:

$$\tilde{\Delta} = (1 - \beta)/\tilde{\alpha} = \Delta\left(1 + 0.86C\frac{(1-\nu^2)\eta V}{aE}[\xi_c(\phi)]^{-5/2}\right). \quad [58]$$

Now let us consider the effect of deformation on the nonhydrodynamic component of interaction. For undeformed spherical particles the force of interaction, F, is related to the force of interaction per unit area of flat plates, Π, according to the Derjaguin formula (39), which is analogous to Eq. [51],

$$F(h) = \pi a \int_h^\infty \Pi(H)dH, \quad [59]$$

while for deformed particles in the limit $u \to 0$ we have

$$\tilde{F} = F + \Delta F, \quad [60]$$

where the correction to the force is given by

$$\Delta F = \pi a \int_h^\infty \frac{d\Pi(H)}{dH} u(\sqrt{a(H-h)})dH \quad [61]$$

and the deformation in the general case is written as $u(r) = u_h(r) + u_{VdW}(r) + u_s(r)$, where $u_{VdW}(r)$ and $u_s(r)$ are the contribution into the deformation due to Van der Waals attraction and biospecific forces. Equations [59]–[61] should be applied both to the forces of Van der Waals attraction ($F \to F_{VdW}$, $\Delta F \to \Delta F_{VdW}$, $\Pi \to \Pi_{VdW}$) and to biospecific forces ($F \to F_s$, $\Delta F \to \Delta F_s$, $\Pi \to \Pi_s$). Recall that Π_s is given by Eq. [24], while for Π_{VdW} we have the well known equation (39)

$$\Pi_{VdW}(H) = -\frac{A}{6\pi H^3}. \quad [62]$$

The hydrodynamic component of deformation is calculated according to Eq. [38], while analogous equations for u_{VdW} and u_s are obtained by substituting Π_{VdW} and Π_s into [38] instead of p.

Let us first consider the system without biospecific interactions, in which particles' capture can be attributed solely to the Van der Waals attraction. We have

$$u_{VdW} = -\frac{1-\nu^2}{E}\frac{A}{a^2}\xi^{-5/2} f_{VdW}(r/\sqrt{ah}), \quad [63]$$

where

$$f_{VdW}(\zeta) = \frac{4}{3\pi^2}\int_0^\infty K\left(\frac{2\sqrt{\zeta'\zeta}}{\zeta'+\zeta}\right)\frac{\zeta' d\zeta'}{(\zeta'+\zeta)(1+\zeta'^2)^3}. \quad [64]$$

Now we make use of [40], [62], and [63] and substitute $u = u_h + u_{VdW}$ into [61]. We find that

$$\frac{\Delta F_{VdW}}{F_{VdW}} = \frac{1-\nu^2}{E}\left(C_1\frac{\eta V}{a}\xi^{-5/2} + C_2\frac{A}{a^3}\xi^{-7/2}\right), \quad [65]$$

where C_1 and C_2 were calculated numerically,

$$C_1 = 6\int_1^\infty \frac{f_h(\sqrt{\zeta-1})}{\zeta^4}d\zeta = 7.5,$$

$$C_2 = 6\int_1^\infty \frac{f_{VdV}(\sqrt{\zeta-1})}{\zeta^4}d\zeta = 0.56. \quad [66]$$

Making use of [66] we are now able to generalize the capture criterion [12] for elastically deformable particles substituting $\tilde{\alpha}$, $\tilde{\Delta}$, and $\tilde{C}_A$ instead of α, Δ, and C_A, where

$$\tilde{C}_A = C_A\left(1 + \frac{1-\nu^2}{E}\left(C_1\frac{\eta V}{a}\xi_c(\phi)^{-5/2} + C_2\frac{A}{a^3}\xi_c(\phi)^{-7/2}\right)\right). \quad [67]$$

In Fig. 11 the effect of deformation on capture efficiency is demonstrated for particles with different Young moduli.

The capture efficiency for particles interacting via the su-

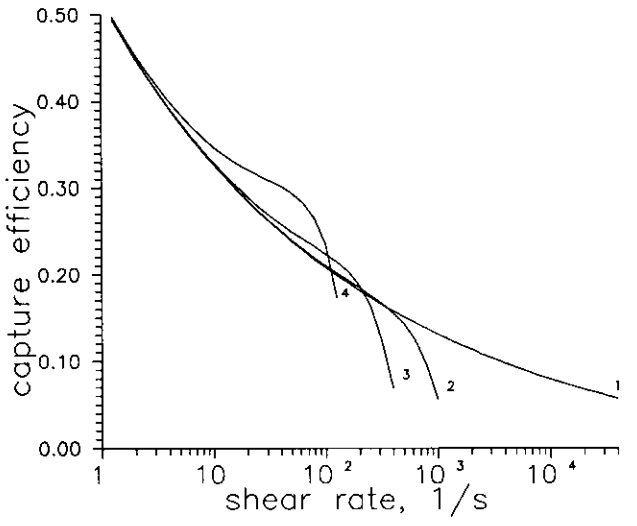

FIG. 11. Capture efficiency for particles interacting via molecular attraction is plotted vs shear rate. Curve (1) is calculated for rigid particles. Curves (2)–(4) are calculated for deformable particles at E (Pa) = 10^8 (2), 10^7 (3), and 10^6 (4). Other parameters are $a = 1$ μm, $A = 10^{-21}$ J, $\eta_0 = 1$ mPa·s.

perposition of Van der Waals attraction and biospecific forces can also be calculated in the framework of our model. To do this we make use of an important simplification, which is based on the decoupling of the contributions of Van der Waals attraction and biospecific interactions. As shown in Fig. 4, biospecific interactions are relevant for the capture only in some clearly defined range of shear rates, such that in this interval the capture process is guided solely by biospecific interaction, while beyond this interval the process of capture is guided solely by Van der Waals attraction. Hence, it is sufficient to calculate the correction to the force of Van der Waals attraction due only to u_h and u_{vdw} (neglecting u_s), while the correction to the force of biospecific interaction can be calculated by taking into account u_h and u_s (not u_{vdw}). It should be also noted that since the biospecific interactions contribute only in a narrow range of ξ (see Eq. [32]), i.e., at $\xi \to \xi_0$, it is sufficient to calculate ΔF_s and u_s at $\xi \to \xi_0$. We have

$$u_s(\xi \to \xi_0) = -\frac{1-\nu^2}{E}[L]_0 a^2 \delta \xi_0 f_s(r/\sqrt{ah}, \epsilon), \quad [68]$$

$$f_s(\zeta, \omega) = \frac{16}{\pi}\int_0^\omega K\left(\frac{2\sqrt{\zeta'\zeta}}{\zeta'+\zeta}\right)\frac{\zeta'^3 d\zeta'}{(\zeta'+\zeta)}, \quad [69]$$

where $\omega \equiv (\Delta/\xi_0)^{1/2}$. Equations analogous to [65]–[67] now take the form

$$\frac{\Delta F_s}{F_s} = \frac{1-\nu^2}{E}\left(C_3(\omega)\frac{\delta a \eta V}{U_a} + C_4(\omega)\frac{[L]_0\delta^2 a^3}{U_a}\right), \quad [70]$$

where

$$C_3(\omega) = 2\int_0^\omega f_h(\zeta, \omega)\zeta d\zeta - \omega f_h(\omega, \omega),$$

$$C_4(\epsilon) = 2\int_0^\omega f_s(\zeta, \omega)\zeta d\zeta - \omega f_s(\omega, \omega), \quad [71]$$

$$\tilde{C}_A = C_A\left(1 + \frac{1-\nu^2}{E}\left(C_3(\omega)\frac{\delta a \eta V}{U_a} + C_4(\omega)\frac{[L]_0\delta^2 a^3}{U_a}\right)\right). \quad [72]$$

Numerical calculations have shown that the functions $C_3(\omega)$ and $C_4(\omega)$ can be well approximated as

$$C_3(\omega) = 0.79\omega^{3.4}, \quad C_4(\omega) = 0.36\omega^{5.0}. \quad [73]$$

In Fig. 12 we plot the dependence of capture efficiency upon shear rate at different Young moduli.

One can see that deformation increases capture efficiency at low shear rates and reduces it at high shear rates. To understand these effects one should recall that there are two

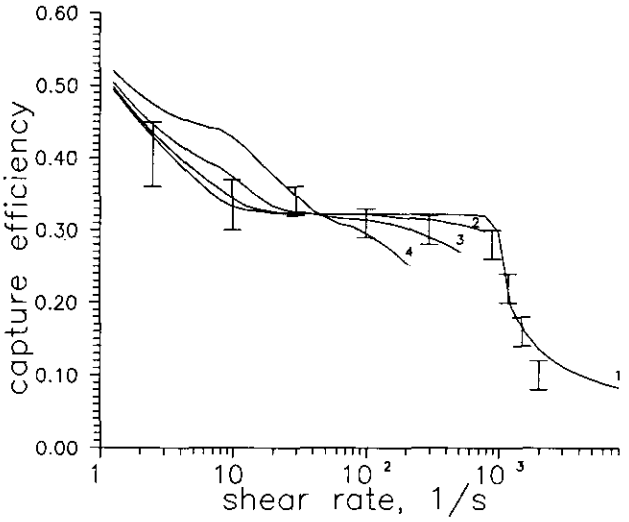

FIG. 12. Capture efficiency for particles interacting via superposition of molecular attraction and biospecific interaction is plotted vs shear rate. Curve (1) is calculated for rigid particles. Curves (2)–(4) are calculated for deformable particles at E (Pa) = 10^6 (2), $3\cdot10^5$ (3), and 10^5 (4). Other parameters are the same as in Fig. 4.

principal ways in which deformation affects the process of coagulation. First, deformation increases the force of attraction which holds the doublet together due to the decrease of the actual gap width between surfaces of particles at given distances between their centers (Eqs. [65] and [70]). Second, it perturbs the trajectories of particles so that the distance between the centers of particles in the stretched doublet is increased (see Eqs. [57], [58]). The first effect dominates at low shear rates, increasing the capture efficiency, while the second effect dominates at high shear rates, decreasing it.

Comparing Figs. 11 and 12 one can see that the effect of deformation on the capture of particles interacting via Van der Waals attraction alone is more significant than its effect on biospecifically interacting particles. The capture of particles interacting via pure Van der Waals attraction is affected by their deformation even if the Young modulus of particles is rather high (at $E = 10^8$ Pa·s the capture efficiency is affected by deformation at G higher than some critical value $G_c \sim 200\ s^{-1}$). As E decreases, G_c also slowly decreases. The capture efficiency of biospecifically interacting particles in the range of shear rates 10–$10^3\ s^{-1}$ is not essentially affected by deformation at $E \geqslant 10^7$ Pa·s, while at lower E capture efficiency in this range of shear rate roughly decreases.

5. COMPARISON WITH THE EXPERIMENTS

In this section some experimental results are discussed which illustrate our theoretical analysis. In our experiments we determined the capture efficiency of platelets in suspension subject to shear flow. The suspension was a platelet-

rich blood plasma without erythrocytes. A detailed description of the procedure of our experiments will be given in Ref. (42).

Platelet aggregation in suspension is a complex and multistage process. It involves three conventional stages:

(i) Addition of a chemical reagent (inductor), which activates platelets, into the platelet rich plasma (PRP). Intracellular cytoskeletal structures undergo changes during the activation which lead to a change in the cellular shape (partially spherical shape). Protein receptors R (glycoprotein IIb/IIIa) located on platelet surface acquire the ability to bind adhesive plasma protein fibrinogen.

(ii) Binding of fibrinogen molecules to a part of surface receptors determined by the chemical equilibrium of the receptor–fibrinogen reaction. As a consequence adhesive receptor–fibrinogen complexes are formed (the analog used in our model of coreceptor (L). It is known that due to several adhesive sites located on fibrinogen molecule, fibrinogen acts as interplatelet bridges binding cells into aggregates.

(iii) Interaction of platelets, having free activated receptors (R) and adhesive receptor–fibrinogen complexes (L) on their surface, in a shear flow; formation of doublets, triplets and so on.

In our experiments donor blood was obtained from healthy men (up to 35 years old) by ulna vein puncture and then stabilized with a 3.8% solution of sodium citrate in a 9:1 ratio. PRP was obtained by blood centrifugation at 110 g for 15 min at room temperature. Platelet concentration in PRP was assayed by the microscopic method. All the experiments were performed within 3–4 h after the blood had been obtained.

The aggregation was studied in the standard viscosity metric cell (the Couette flow). A He–Ne laser was used as a probe, its radiation was directed between the cylinders of the cell parallel to the rotation axis. The light was recorded with a photodiode detector. Adenosine diphosphate (ADP) at the concentration 20 μM was used as an inductor of aggregation.

The experimental procedure was as follows. The PRP suspension, sheared between two cylinders at $G = 10^2\ s^{-1}$ in the cell, was supplemented with ADP in the corresponding concentration. In 5–7 s the procedure was stopped. In 25–30 s the procedure was resumed at the studied shear rate. According to Ref. (43) during this period platelets have been completely activated and their shape changed, whereas the aggregation due to the Brownian diffusion and binding of fibrinogen molecules (formation of coreceptors) for 30–40 s can be neglected (42, 44, 45). Thus, in our system one can assume $[R]_0$ to be much greater than $[L]_0$, as we did above. After shear is resumed, the initial rate of increase of transmitted light intensity, D_0, related to difference between light intensities for platelet pure and rich plasma was recorded. The parameter D_0 is widely used in medicine. It characterizes the intensity of formation of small aggregates, primarily cell doublets. For shear rates $G > 10\ s^{-1}$, at which the shear platelet aggregation essentially predominates over the Brownian aggregation (44), D_0 may be assumed to equal $J/2$ (42, 46). With average radius of platelets taken to be equal to 1 μm (see (43)), from Eq. [1] an experimental capture efficiency is determined. The typical experimental data for PRP are given in Figs. 5–8 and 12.

Let us now compare our experimental data with the theoretical calculations of the capture efficiency dependence upon shear rate. In Figs. 5–8 the results of these calculations are plotted for particles interacting via superposition of Van der Waals attraction and biospecific forces. This seems to be a reasonable model for interaction of platelets in blood plasma in shear flow. Electrostatic barriers due to high electrolyte concentration in plasma are essentially suppressed. The best correlation between theoretical and experimental data is obtained at $\xi_0 = 0.03$, $\delta = 10^{-2}$ N/m. These values are quite reasonable for biological cells (9, 14, 34).

Comparing our experimental data with the results of calculations of the capture efficiency of deformable particles plotted in Fig. 12, we conclude that the Young modulus of platelets E should be high enough, $E \geqslant 10^6$ Pa. The agreement with the experimental data achieved at $E = 3 \cdot 10^5$–10^6 Pa seems to be somewhat better than that for rigid particles (the curve becomes smoother at the edge of the plateau). However, further experiments are necessary to make a decisive conclusion concerning the effect of deformation on coagulation.

6. CONCLUSION

In this paper an approximate method is developed for determination of the capture efficiency of particles in shear flow. The method makes it possible to describe the coagulation of particles with different types of attractive interaction.

In the first stage of our analyses we consider an idealized system, in which the nonhydrodynamic interaction is reduced to Van der Waals attraction. For such a system calculations of capture efficiency in terms of our simplified analysis have been shown to be in good agreement with those carried out by other authors on the basis of analysis of numerically calculated trajectories. Our approach also makes it possible to take into account the corrections to capture efficiency due to elastic deformation of particles.

In the second stage of our analyses consider applications of our model to the coagulation of biological cells, such as activated platelets (i.e., blood cells, which are responsible for thrombous formation). In the first approximation we described the cells as spherical elastic particles interacting via the superposition of Van der Waals attraction and biochemically specific forces, which are attributed to receptor–coreceptor bonds between cells' surfaces. For such a system we found that the capture efficiency as a function of shear rate,

$\epsilon(G)$, is essentially different from the one for idealized system which had been considered on the first stage. Specific interactions lead to increase in capture efficiency at intermediate shear rate, so that a "plateau" appears on the curve $\epsilon(G)$. This type of the dependence is in agreement with the one observed for blood platelets aggregation. Corrections due to deformation lead to a certain decrease in ϵ at high shear rate and its increase at low shear rate.

Further analysis of this problem should be carried out taking into account a number of additional factors which affect adhesive cell–cell interactions, e.g., the effect of steric stabilization due to the long-chain polysaccharide molecules (glycocalix) on the surfaces of biological cells (5, 27). Further development of our approach may also include some modifications of the mechanical model of the cell, e.g., by introduction of viscoelastic membrane on its surface with bending rigidity and surface tension. This approximation is relevant to large cells such as lymphocytes and erythrocytes.

REFERENCES

1. Woodruff, J. J., Clarke, L. M., and Chin, Y. H., *Ann. Rev. Immunol.* **5,** 201 (1987).
2. Nicholson, G. L., *Exp. Cell Res.* **150,** 3 (1984).
3. Berenson, R. J., Bensinger, W. I., and Kalamasz, D. J., *Immunol. Meth.* **91,** 11 (1986).
4. Jarrel, B. E., Williams, S. K., Solomon, L., Speicher, L., Koolpe, E., Radomski, R. A., Carabasi, R. A., Greener, D., and Rosato, F. E., *Ann. Surg.* **203,** 671 (1986).
5. Bongrand, P., and Bell, G. I., *in* "Cell Surface Dynamics" (C. DeLisi, A. Perelson, and F. Wiegel, Eds.), p. 459. Dekker, New York, 1984.
6. Mustard, J. F., and Packham, M. A., *Thromb. Diath. Haemorrh.* **33,** 444 (1975).
7. Karino, T., and Goldsmith, H. L., *in* Haemostasis and Thrombis" (A. L. Bloom and D. P. Thomas, Eds.), p. 739. Churchill Livingstone, London, 1987.
8. Tozeren, H., and Skalak, R., *J. Fluid Mech.* **95,** 743 (1979).
9. Beier, P. W., "Biophysik. Eine Einfuhrung in die Physikalische Betrachtungsweise der Eigenschaften und Funktionen Leben der Systeme." Veb Georg Thieme, Leipzig, 1960.
10. Von Smoluchowksi, M., *Z. Phys. Chem.* **92,** 129 (1917).
11. Van de Ven, T. G. M., and Mason, S. G., *Colloid Polym Sci.* **255,** 468 (1977).
12. Zeichner, G. R., and Schowalter, W. R., *AIChE J.* **23,** 243 (1977).
13. Potanin, A. A., *J. Colloid Interface Sci.* **145,** 140 (1991).
14. Verkhusha, V. V., Vrzheshch, P. V., Staroverov, V. M., and Varfolomeev, S. D., *J. Chem. Biochem. Kinet.* **2,** 214 (1992).
15. Serayssol, J.-M., and Davis, R. H., *J. Colloid Interface Sci.* **114,** 54 (1986).
16. Davis, R. H., Serayssol, J.-M., and Hinch, E. J., *J. Fluid Mech.* **163,** 479 (1986).
17. Batchelor, G., and Green, J. T., *J. Fluid Mech.* **56,** 375 (1972).
18. Bell, G. I., *Science* **200,** 618 (1978).
19. Berg, H. C., and Purcell, E. M., *Biophys. J.* **20,** 193 (1977).
20. Dembo, M., Goldstein, B., Sobotka, A. K., and Lichtenstein, L. M., *J. Immunol.* **122,** 518 (1979).
21. DeLisi, C., *Mol. Immunol.* **18,** 507 (1981).
22. DeLisi, C., *in* "Cell Surface Dynamics" (A. Perelson, C. DeLisi, and F. Wiegel, Eds.), p. 205. Dekker, New York, 1984.
23. Torney, D. C., and McConnell, H. M., *Proc. R. Soc. London A* **387,** 147 (1983).
24. Adam, G., and Delbruck, M., *in* "Structural Chemistry and Molecular Biology" (A. Rich and N. Davidson, Eds.), p. 198. Freeman, San Francisco, 1968.
25. Axelrod, D., Koppel, D. E., Schlessinger, J., Elson, E., Webb, W. W., and Podleski, T. R., *Biophys. J.* **16,** 1055 (1976).
26. Saffman, P. G., *J. Fluid Mech.* **73,** 593 (1976).
27. Saffman, P. G., and Delbruck, M., *Proc. Natl. Acad. Sci. U.S.A.* **72,** 3111 (1975).
28. Wiegel, F. W., *in* "Cell Surface Dynamics" (A. Perelson, C. DeLisi, and F. Wiegel, Eds.), p. 135. Dekker, New York, 1984.
29. DeLisi, C., *Q. Rev. Biophys.* **13,** 201 (1980).
30. Bell, G. I., Dembo, M., and Bongrand, P., *Biophys. J.* **33,** 1051 (1984).
31. Belintsev, B. N., *Biol. Membr.* **5,** 1100 (1988). [In Russian]
32. Hill, T. L., *Prog. Biophys. Mol. Biol.* **28,** 267 (1974).
33. Levy, R. M., and Karplus, M., *Biopolymers* **18,** 2465 (1979).
34. Tozeren, A. J., *Theor. Biol.* **140,** 1 (1989).
35. Pecht, I., and Lancet, O., *in* "Chemical Relaxation in Molecular Biology" (I. Pecht and R. Ringler, Eds.). Springer-Verlag, New York, 1977.
36. Tozeren, A., Sung, K.-L.P., and Chien, S., *Biophys. J.* **55,** 479 (1989).
37. Abbott, A. J., and Nelsestuen, G. L., *FASEB J.* **2,** 2858 (1988).
38. Wiley, H. S., *Curr. Top. Membr. Transp.* **24,** 369 (1985).
39. Derjaguin, B. V., Churaev, N. V., and Muller, V. M., "Surface Forces." Moscow, Nauka, 1986. [In Russian]
40. Van de Ven, T. G. M., and Mason, S. G., *J. Colloid Interface Sci.* **57,** 517 (1976).
41. Landau, L. D., and Lifshitz, E. M., "Theory of Elasticity." Moscow, Nauka, 1969. [In Russian]
42. Verkhusha, V. V., Lebedev, Ye. S., and Vrzheshch, P. V., submitted for publication.
43. Bell, D. N., Spain, S., and Goldsmith, H. L., *Biophys. J.* **56,** 817 (1989).
44. Frojmovic, M., Longmire, K., and Van de Ven, T. G. M., *Biophys. J.* **58,** 309 (1990).
45. Peerschke, E. I. P., *Semin. Hematol.* **22,** 241 (1988).
46. Hantgan, R. R., *Biochim. Biophys. Acta* **846,** 64 (1985).